J Mater Sci (2006) 41:7374–7379
DOI 10.1007/s10853-006-0813-1

The structural and electrical properties of nano-scale Sr_2FeMoO_6 under high pressures

P. E · J. S. Zhang · L. D. Yao · F. Y. Li · Z. X. Bao · J. X. Li · Y. C. Li · J. Liu · C. Q. Jin · R. C. Yu

Received: 8 November 2004 / Accepted: 5 December 2005 / Published online: 19 September 2006

Abstract Using the polymer-network gel method to control the chemical procedure, Sr_2FeMoO_6 powders with grain size of 50 nm (A) and 100 nm (B) have been synthesized, and their structural and electrical properties have been investigated. By comparing the experimental results of samples A and B with that of bulk sample C with grain size in μm obtained before, sample A shows the largest bulk modulus B_0 and a relatively large slope of the drop in resistance as a function of pressure. The possible reasons are given and discussed.

Introduction

The colossal magnetoresistance (CMR) in doped pervoskite manganates has attracted great attention of scientists due to its possible technological applications [1]. Recently, interest has been focused on the magnetotransport properties of the double pervoskite Sr_2FeMoO_6 due to its large magnetoresistance (MR) at room temperature and high Curie temperature of 410–450 K [2, 3]. A noteworthy feature of these materials is the high-degree spin polarization of the charge carriers, caused by the half-metallic nature of the materials [4, 5]. In some previous work on Sr_2FeMoO_6 [6–10], low-field spin-polarized intergrain tunneling magnetoresistance (IMR) has been observed. Furthermore, it has been proven that it is very effective to enhance the low-field IMR at room temperature by reducing the size of the crystalline grains, considering that the IMR is closely related to the grain boundaries. In this paper, we report the study on two polycrystalline Sr_2FeMoO_6 samples with 50 and 100 nm prepared by polymer-net gel method, concerning the structural instability and electrical properties under high pressure up to 38.5 and 20 GPa, respectively. The results obtained will be compared with that of Sr_2FeMoO_6 with grain size in μm synthesized by traditional solid-state reaction. The structural stability of different size Sr_2FeMoO_6 compounds under high pressure has also been investigated with a diamond anvil cell (DAC) by energy dispersive X-ray diffraction with synchrotron radiation. It is believed that these works will be instructive for the relative further study on IMR of double perovskite compounds with nano-scale grains.

Experiments

Polycrystalline ordered double-perovskite Sr_2FeMoO_6 powders with different grain sizes were prepared by a polymer-network gel method [11–13] followed by heat treatment. According to the formula Sr_2FeMoO_6, stoichiometric amounts of $Fe(NO_3)_3{\cdot}9H_2O$, $Sr(NO_3)_2$

P. E · J. S. Zhang · L. D. Yao · F. Y. Li · Z. X. Bao · C. Q. Jin · R. C. Yu (✉)
Beijing National Laboratory for Condensed Matter Physics, Institute of Physics, Chinese Academy of Sciences, P.O. Box 603, Beijing 100080, P.R. China
e-mail: rcyu@aphy.iphy.ac.cn

J. X. Li · P. E
State Key Laboratory of Inorganic Synthesis and Preparative Chemistry, Jilin University, Changchun 130012, P.R. China

Y. C. Li · J. Liu
Institute of High Energy Physics, Chinese Academy of Sciences, Beijing 100039, P.R. China

and $(NH_4)_6Mo_7O_{24}{\cdot}4H_2O$ were dissolved in deionized water containing citric acid to form a uniform solution. After the pH value was regulated with ammonia, polymerization agents and starters were added to the solution. Keeping the temperature at 80 °C for a few minutes, the solution polymerized into polymer gel. The gel was crushed, dried at 120 °C, then fired at 500 °C in an oxygen atmosphere to convert the gel into superfine powders. Finally, the powders were pelletized, heated at 700 °C for 6 h in a mixed gas stream of 1% H_2/Ar and cooled down in situ to room temperature to yield the required product. Solutions with different concentrations will produce the compounds with different sizes.

The crystal structure and phase purity of the samples were examined by X-ray powder diffraction with CuKα radiation at ambient temperature. The in situ high pressure energy dispersive X-ray diffraction experiments on Sr_2FeMoO_6 were carried out in a DAC, with a culet of 480 μm in diameter, using synchrotron white radiation at the Beijing Synchrotron Radiation Facility (BSRF). The size of X-ray spot was 80 × 80 μm. The powders of samples were mixed with a suitable amount of Au powders for inner pressure calibration, and loaded into a hole 300 μm in diameter in a T301 stainless-steel gasket. In this experiment, the relation between the energy and channel number is $E = 0.77788(\text{keV}) + 0.01041(\text{keV})*\text{chn}$, here chn stands for the sequencial number of the channel from 1 to 4096. According to the formula $\sin\theta = \frac{0.619925}{[d(\text{nm})\times E(\text{keV})]}$, the diffraction angle θ =7.0294° was obtained for E = 21.51 keV and d = 0.2355 nm for the Au (111) peak.

Samples were also examined in a DAC, using resistance and capacitance measurements, as reported previously [14], to obtain the resistance versus pressure (R–P) and the capacitance versus pressure (C–P) curves. The resistance and capacitance measurements were performed on a ZL5 intelligent LCR system at 1 kHz. Figure 1 shows the schematic diagram of the molybdenum electrodes placed on the lower diamond anvil. Two parallel Mo sheets were used as electrodes of a capacitor, and also as the probes in resistance measurements. There are two leads for each electrode: one of them is used for the current and the other for voltage measurement (1, 4 and 2, 3 are used for current and voltage, respectively). The Mo electrodes were made by photoetching them away from a base plate, which was a phenolic methylal glue film with a thickness of 0.04 mm. The electrode thickness ranges from 0.008 to 0.010 mm, while the distance between the two electrodes is 0.03 to 0.05 mm. The Sr_2FeMoO_6 powder was put between the electrodes as a medium. From the above descriptions, it is evident that the geometry of the device is far from an ideal parallel-plate capacitor, but it can be used to detect the capacitance changes associated with phase transitions. The LCR meter calculates and gives the R and C values simultaneously according to the data measured in the experiments. The samples studied were pre-pressed under 4.0 GPa to make them compact enough for the measurement.

The grain size and its morphology of the samples were also checked with an XL30 S-FEG scanning electron microscope (SEM).

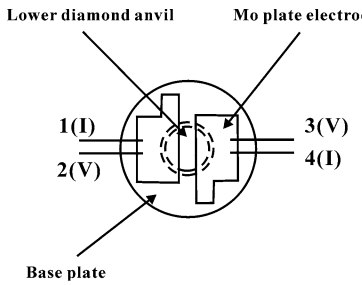

Fig. 1 Top view of Mo electrodes placed on the lower diamond anvil

Results and discussion

The polymer-network gel method is a suitable way to prepare high-purity Sr_2FeMoO_6 powders, in which the chemical processes can control the particle size. Two kinds of Sr_2FeMoO_6 polycrystals A (50 nm) and B (100 nm) have been successfully synthesized.

Figure 2 is the XRD patterns of the synthesized samples A and B at ambient temperature. They show a

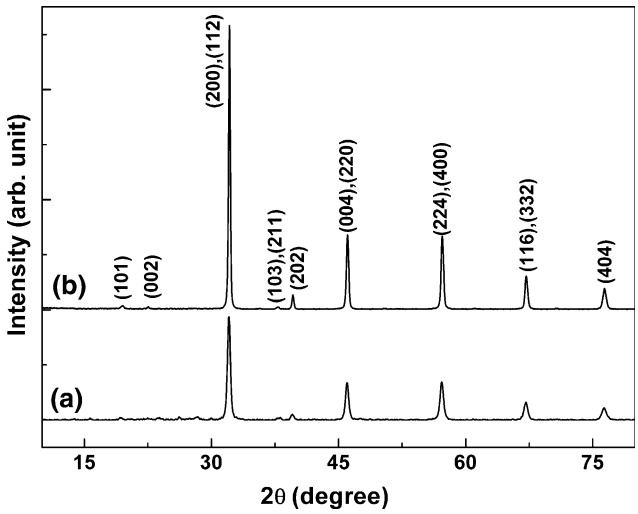

Fig. 2 The XRD patterns of the synthesized Sr_2FeMoO_6 with different grain sizes, (**a**) for A with 50 nm and (**b**) for B with 100 nm. The peaks are index in a tetragonal structure with a space group I4/mmm

clean single phase without detectable impurities. The diffraction peaks are indexed in a tetragonal structure with a space group I4/mmm. The lattice parameters have been refined from XRD data, leading to a = 5.5703 Å, c = 7.8832 Å for sample A and a = 5.5791 Å, c = 7.8698 Å for sample B, which are similar to the result of polycrystalline bulk sample C (a = 5.5703 Å, c = 7.7879 Å) with grains of a size of 2 μm [15]. Evidently, the width at half height of line (200) of sample A is broader than that of sample B, showing that the grain size of sample A is smaller than that of sample B. According to the Scherrer formula $D_{hkl} = k\lambda/\beta \cos\theta$, where D_{hkl} is the diameter of the particle, k is a constant, β is the difference of the widths at half height of the peak between the measured sample and the standard of KCl used to calibrate the width of the sample and λ is the wavelength of the X rays used, the average grain sizes obtained are about 50 and 100 nm for samples A and B, respectively. The results have been strongly supported by SEM observations of the as-prepared samples shown in Fig. 3. It can be seen clearly that the grain size of sample A is smaller than that of sample B. Moreover, the particles are uniform and fine in the whole region. The chemical composition of the samples has been checked by energy dispersive X-ray microanalysis in situ in a SEM and determined to be close to Sr_2FeMoO_6 besides a little impurity of carbon element.

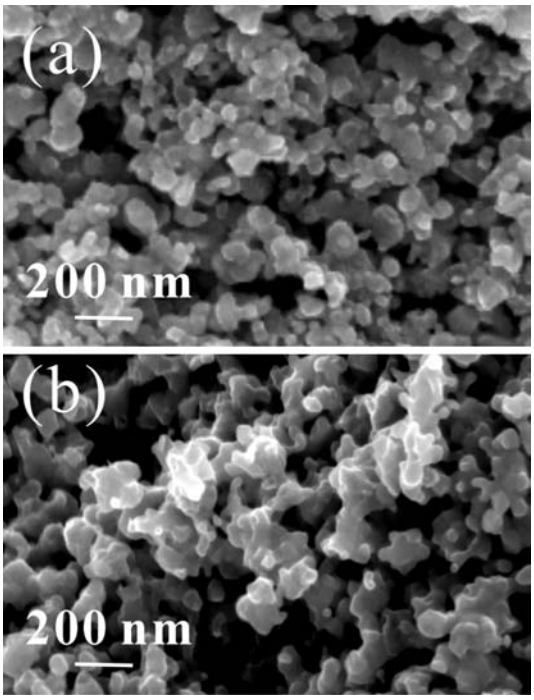

Fig. 3 SEM images of samples A and B, (**a**) for A with 50 nm and (**b**) for B with 100 nm

The energy dispersive X-ray diffraction patterns of samples A and B at different pressures obtained at room temperature are shown in Fig. 4. In our experiments, the applied maximum pressure is 32.5 and 35 GPa for samples A and B, respectively. Obviously, the variations of the patterns of sample A are rather similar to those of sample B as well as that of sample C reported in Ref. 15. Therefore, we will analyze the patterns of sample A qualitatively to give an account of the similarity of sample B. Figure 4 shows that the sample peaks indexed at the starting pattern obtained at ambient pressure will shift with increasing pressure due to the compression of the unit cell. Furthermore, all the diffraction peaks become weakened and even vanish with increasing pressure since some portion of the sample may flow out of the sample chamber during the experiments. It should be noted that the broadening of the peaks with increasing pressure indicates a pressure gradient in the sample. When the pressure is decreased to ambient, the sample peaks will move back to the original positions. In the experiments, due to the constant value of $E \times d$, the d values of the sample

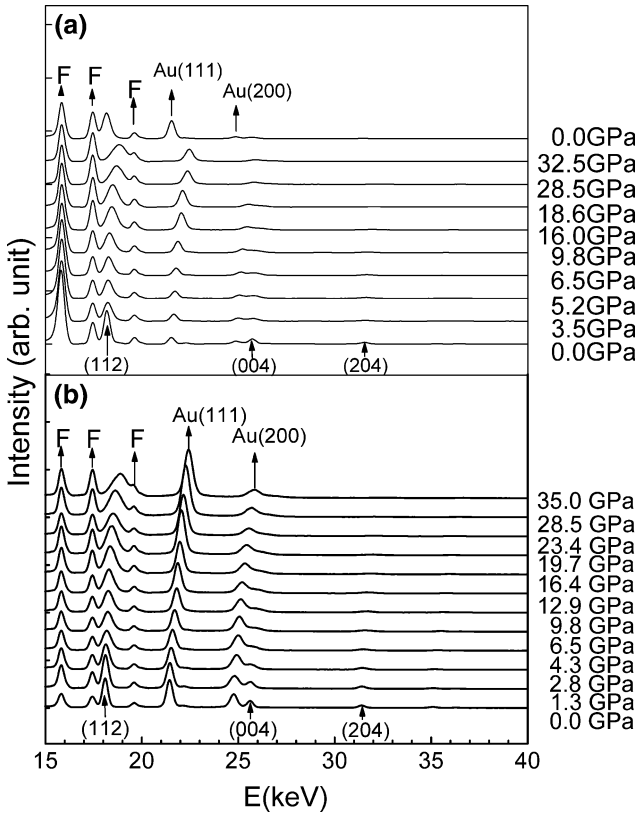

Fig. 4 (**a**, **b**) The energy dispersive X-ray diffraction patterns of samples A and B at different pressures, respectively. The sample peaks are indexed at the starting pattern obtained at ambient pressure and the peaks marked as F are the fluorescence peaks of the elements in the sample

peaks were calculated through the E values of the peak positions. In addition to the sample peaks and Au peaks, some fluorescence peaks of the elements in the sample appear in the patterns and are marked as F, but they do not change their positions with pressure since the pressure we used is too low to change the energy levels of the shells or sub-shells. No new diffraction peaks have been detected in the experiments, suggesting that the crystal structure of samples A and B is stable in the range of pressure studied. These results show that the structural stability of nano-scale Sr_2FeMoO_6 is similar to that of bulk polycrystalline one [15].

From Fig. 4 the cell parameter and cell volume are calculated at each pressure and the V/V_o–P curves for samples A and B are presented in Fig. 5. The experimental data are fitted using the Birch–Murnaghan (BM) equation [16], by assuming that the isothermal bulk modulus B varies linearly with pressure, i.e. $B = B_0 + B_0'P$,

$$P(\mathrm{GPa}) = \frac{3}{2} \times B_0 \times \left[\left(\frac{V_0}{V}\right)^{\frac{7}{3}} - \left(\frac{V_0}{V}\right)^{\frac{5}{3}} \right] \times \left\{ 1 - \left(3 - \frac{3}{4} \times B_0'\right) \times \left[\left(\frac{V_0}{V}\right)^{\frac{2}{3}} - 1 \right] \right\},$$

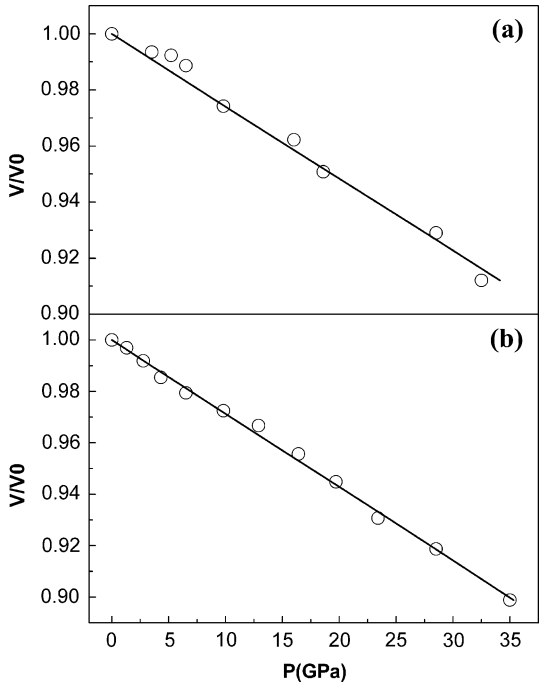

Fig. 5 (**a**, **b**) V/V_0–P relationships for Sr_2FeMoO_6 samples with grain sizes in 50 nm and 100 nm, respectively. The open circles represent the experimental data and the solid lines represent the fitting curves

where V_0 and V are the volumes at ambient and high pressure P, respectively. We obtain the isothermal bulk modulus at ambient pressure B_0, assuming its first-order derivative $B_0' = 4$. For comparison, the B_0 values of samples A and B with nano-scaled grain sizes and that of sample C with grain size in μm are listed in Table 1. It can be found that the value of B_0 increases with decreasing grain size. The possible explanation of the B_0 values in different samples is given as follows. As is well known, there exist a lot of boundary volumes in the nano-scaled materials and some of the atomic arrangements are disordered in the grain boundaries. Moreover, the atoms in nanocrystals tend to vibrate at low frequencies [17, 18]. When a pressure is applied to the nano-scaled materials, it first compresses the grain boundary volumes, changes the shape of the nanocrystals and prevents the atoms from vibrating, and then compresses the unit cell of the nanocrystals. In other words, part of the pressure will act on the grain boundary areas and change the shape of the nanocrystals to bring about a tighter connection between crystal grains. The bulk modulus B_0 deduced from the energy dispersive X-ray diffraction reflects the inner changes in the nanocrystal structure. Therefore, the sample with grain size in nm shows a larger B_0, that is to say, the sample needs a higher pressure to introduce corresponding changes as compared with the sample with grain size in μm because more grain boundary areas exist in the nano-scaled samples. So it is easily understood that the value of B_0 keeps increasing with the decrease of grain size.

Crystal structure change or electronic structure change of the samples will affect the electrical properties of the samples. So it is very helpful to study the change of resistance and capacitance versus pressure to obtain some transition information of the samples. Figures 6a, b present the pressure dependences of resistance $R(P)$ and capacitance $C(P)$ for samples A and B, respectively. In Fig. 6a, the resistance decreases very little in the pressure range of 0 ~ 2.14 GPa and then drops abruptly in the range of 2.14 ~ 6.07 GPa, followed by a slow decrease up to 20 GPa. Similar to the R–P curve, the capacitance rises abruptly also in the pressure range of 2.14 ~ 6.07 GPa in the simultaneous measurements. Sample B shows similar behavior (Fig. 6b) to sample A except for a little deviation of pressure range where the resistance and capacitance

Table 1 B_0 values of samples A and B with grain size in nm and that of sample C with grain size in μm

Samples	A (50 nm)	B (100 nm)	C (~μm)
B_0 (GPa)	331 ± 12	284 ± 6	266 ± 3

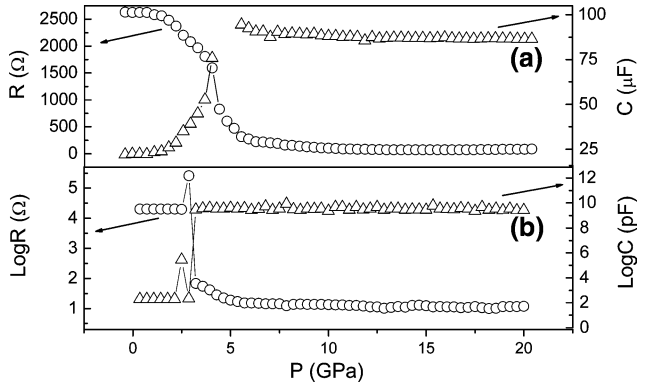

Fig. 6 (**a**, **b**) The pressure dependences of resistance and capacitance for A and B at room temperature, respectively

changes occur. In the previous work, the transition pressure of sample C has also been found at about 2.1 Gpa [15]. It should be indicated that there are large differences in the resistance and capacitance values among samples A, B and C at ambient pressure, as well as in their magnitudes of change at the transitions. Some experimental data of capacitance for sample A may even be undetectable due to the limitation of measurement range of the instrument. We think one possible reason is that there are more grain boundary areas for the small grain sized sample, so sample A shows larger resistance than sample B. Another possible reason is that different R and C values may be caused by the different amounts of the powders used in the measurements. However, the differences in their values do not affect the determination of the transition pressures we want to determine. Based on the results of energy dispersive X-ray diffraction, the abrupt drop of resistance and sharp increase of capacitance in the measurements can be attributed to the electronic structure change, which is caused by the compression of the unit cell under high pressures. These results are very similar to those observed by Zhao et al. in Sr_2FeMoO_6 in μm scale [15]. The unit cell volumes corresponding to the electrical transitions of samples A, B and C are calculated as 243.80, 242.99 and 239.74 $Å^3$, respectively. Though the unit cell volume at the transition decreases a little with increasing grain size of the sample, we still think that the transitions occur in the same range of unit cell volume regardless of the tiny differences. It is very interesting that the drop in $R(P)$ shows a slow change with decreasing grain size. As is well known, the grain boundary area increases with decreasing grain size, which forms more tunneling barriers for carrier transport. As mentioned above, some part of the loaded pressure acts for the compression of the boundary areas in the sample and the distortion of the shape of nanocrystals. These may induce the slow change of the $R(P)$ in the measurement. Moreover, as many novel properties have been found in nano-scaled materials, the half-metal band structure of Sr_2FeMoO_6 will also be influenced by the grain size in nano-scale in addition to the crystal structure. This might be another reason to give rise to the slower drop for the smaller grain size in the R–P measurement. A detailed study in this aspect is underway. The transport property has a close relation with the band structure and the density of states near the Fermi level of materials as well as grain boundary areas. These factors will affect the CMR of the materials that have potential applications in memory devices. Nowadays, memory devices have a trend of being made by nano-scaled materials. As is well known, high pressure has a strong influence on grain boundary areas of nano-scaled materials as well as their crystal structure, and chemical pressure will occur when the cations in CMR compounds are substituted by small ones, so the studies of CMR materials in nano-scale size under high pressure play an important role in investigating and understanding the mechanisms of CMR effect.

Conclusions

The structure stability and electrical properties of Sr_2FeMoO_6 samples A and B with grain size in nm have been investigated using in situ high pressure energy disperse XRD and resistance and capacitance measurements. The results indicate that no crystal structure transition occurs in the whole pressure range studied except for the compression of the unit cell. That is to say, the structure of nano-scale Sr_2FeMoO_6 is stable in the measured pressure range. The bulk modulus, obtained from B–M equation, increases with decreasing particle size. The steep drop of R–P and the abrupt rise of C–P near 2.1 GPa for both samples are considered to be an electronic structural transition due to the compression of the unit cell under pressure. Samples with different grain sizes show different slopes of R–P drop in the measurements. This phenomenon might be caused by the grain boundary effect in the transport and grain size effect in the band structure.

Acknowledgements This work was supported by the National Natural Science Foundation of China (Grant Nos. 50471053, 50321101 and 50332020) and the State Key Development Program for Basic Research of China (Grant No. 2005 CB623602).

References

1. For a review, see Colossal magnetoresistive oxides, edited by Y. Tokura (2000) Gordan and Breach, New York
2. Kobayashi K-I, Kimura T, Sawada H, Terakura K, Tokura Y (1998) Nature 395:667
3. Kim TH, Uehara M, Cheong S-W, Lee S (1999) Appl Phys Lett 74:1737
4. Okimoto Y, Katsufuji T, Ishikawa T, Urushibara A, Arima T, Tokura Y (1995) Phys Rev Lett 75:109
5. Park J-H, Vescovo E, Kim H-J, Kwon C, Ramesh R, Venkatesan T (1998) Nature 392:794
6. Ju KL, Gopalakrishnan J, Peng JI, Li Q, Xiong GC, Venkatesan TV, Green RG (1995) Phys Rev B51:6143
7. Sun JZ, Gallagher WJ, Duncombe PR, Krusin-Elbaum L, Altman RA, Gupta A, Lu Y, Gong GQ, Xiao G (1996) Appl Phys Lett 69:3266
8. Hwang HY, Cheong S-W, Ong NP, Batlogg B (1996) Phys Rev Lett 77:2041
9. Hwang HY, Cheong S-W (1997) Nature 389:942
10. Hwang HY, Cheong S-W (1997) Science 278:1607
11. Yelon WB, Hu Z, James WJ, Marasinger GK (1996) J Appl Phys 79:5939
12. Zhang HW, Zhang SY, Shen BG, Lin C (1999) J Appl Phys 85:4660
13. Lin JH, Liu SF, Qian XL, Su MZ (1996) J Alloys Comp 238:113
14. Bao ZX, Schmidt VH, Howell FL (1991) J Appl Phys 70:6804
15. Zhao P, Yu RC, Li FY, Liu ZX, Jin MZ, Jin CQ (2002) J Appl Phys 92:1942
16. Gerward L (1985) J Phys Chem Solids 46:925
17. Chadi DJ, Martin RM (1976) Solid State Commun 19:643
18. Dougherty TP (1992) Science 258:770